

2006

Dynamics of an Atmospheric Pressure Plasma Plume Generated by Submicrosecond Voltage Pulses


XinPei Lu

Old Dominion University

Mounir Laroussi

Old Dominion University, mlarouss@odu.edu

Follow this and additional works at: https://digitalcommons.odu.edu/ece_fac_pubs

 Part of the [Electrical and Computer Engineering Commons](#), [Engineering Physics Commons](#), and the [Plasma and Beam Physics Commons](#)

Repository Citation

Lu, XinPei and Laroussi, Mounir, "Dynamics of an Atmospheric Pressure Plasma Plume Generated by Submicrosecond Voltage Pulses" (2006). *Electrical & Computer Engineering Faculty Publications*. 15.
https://digitalcommons.odu.edu/ece_fac_pubs/15

Original Publication Citation

Lu, X., & Laroussi, M. (2006). Dynamics of an atmospheric pressure plasma plume generated by submicrosecond voltage pulses. *Journal of Applied Physics*, 100(063302), 1-6. doi: 10.1063/1.2349475

Dynamics of an atmospheric pressure plasma plume generated by submicrosecond voltage pulses

XinPei Lu and Mounir Laroussi

Citation: [Journal of Applied Physics](#) **100**, 063302 (2006); doi: 10.1063/1.2349475

View online: <http://dx.doi.org/10.1063/1.2349475>

View Table of Contents: <http://scitation.aip.org/content/aip/journal/jap/100/6?ver=pdfcov>

Published by the [AIP Publishing](#)

Articles you may be interested in

[Generation of a direct-current, atmospheric-pressure microplasma at the surface of a liquid water microjet for continuous plasma-liquid processing](#)

[J. Vac. Sci. Technol. A](#) **33**, 021312 (2015); 10.1116/1.4907407

[Relation between plasma plume density and gas flow velocity in atmospheric pressure plasma](#)

[Phys. Plasmas](#) **21**, 043511 (2014); 10.1063/1.4873384

[Sharp bursts of high-flux reactive species in submicrosecond atmospheric pressure glow discharges](#)

[Appl. Phys. Lett.](#) **89**, 231503 (2006); 10.1063/1.2397570

[Submicrosecond pulsed atmospheric glow discharges sustained without dielectric barriers at kilohertz frequencies](#)

[Appl. Phys. Lett.](#) **89**, 161505 (2006); 10.1063/1.2361274

[Comparison of atmospheric-pressure helium and argon plasmas generated by capacitively coupled radio-frequency discharge](#)

[Phys. Plasmas](#) **13**, 093503 (2006); 10.1063/1.2355428



NEW Special Topic Sections

NOW ONLINE
Lithium Niobate Properties and Applications:
Reviews of Emerging Trends

AIP | Applied Physics Reviews

Dynamics of an atmospheric pressure plasma plume generated by submicrosecond voltage pulses

XinPei Lu and Mounir Laroussi^{a)}

Reidy Research Center for Bioelectronics, Electrical and Computer Engineering Department, Old Dominion University, Norfolk, Virginia 23529

(Received 23 March 2006; accepted 26 June 2006; published online 21 September 2006)

Nonequilibrium plasmas driven by submicrosecond high voltage pulses have been proven to produce high-energy electrons, which in turn lead to enhanced ionization and excitations. Here, we describe a device capable of launching a cold plasma plume in the surrounding air. This device, “the plasma pencil,” is driven by few hundred nanosecond wide pulses at repetition rates of a few kilohertz. Correlation between current-voltage characteristics and fast photography shows that the plasma plume is in fact a small bulletlike volume of plasma traveling at unusually high velocities. A model based on photoionization is used to explain the propagation kinetics of the plasma bullet under low electric field conditions. © 2006 American Institute of Physics.

[DOI: 10.1063/1.2349475]

INTRODUCTION

Nonequilibrium plasmas, which have a relatively high electron temperature and low gas temperature, have many attractive characteristics. One of them is their enhanced plasma chemistry at relatively low gas temperatures. Their technological applications include the biological and chemical decontaminations of media, surface modification/functionalization of polymers, absorption and reflection of electromagnetic waves, deposition of thin films, the synthesis of carbon nanotubes, and shock-wave mitigation at supersonic speeds.^{1–8}

To drive the electrons' temperature to even higher levels, pulsed electric fields (pulse widths from few to hundreds of nanoseconds) have proven to be a promising means, which can enhance active chemical species generation efficiency and ultraviolet (UV) emission intensity.^{9–12} Recently, we reported on a specially designed cold plasma jet, “the plasma pencil,” which was driven by submicrosecond voltage pulses and was able to generate room temperature plasma plumes up to 5 cm in length.¹³ In this paper, in order to have an in-depth understanding of the characteristics of the plasma plume, first the *I-V* characteristics of the discharge are studied. Then, using a fast charge-coupled device (CCD) camera, the temporal and spatial evolutions of the plasma inside the discharge chamber and in the plume are elucidated. Finally, a model based on photoionization is proposed to explain the high-speed propagation of the plasma plume under low applied electric field conditions.

EXPERIMENTAL SETUP

Figure 1 is a schematic of the experimental setup. Each of the two electrodes is made of a thin copper ring attached to the surface of a centrally perforated alumina (Al_2O_3) disk. The hole in the center of the alumina disk is 3 mm in diam-

eter, while the diameter of the disk is about 2.5 cm. The diameter of the copper ring is greater than that of the hole, but smaller than that of the disk. The two electrodes are inserted in a dielectric cylindrical tube of about the same diameter as the disks and are separated by a gap the distance of which can be varied in the 0.3–1 cm range. The two electrodes are connected to a high voltage pulse generator capable of producing pulses with amplitudes of up to 10 kV, pulse widths variable from 200 ns to dc, and with a repetition rate of up to 10 kHz. The rise and fall times of the voltage pulses are about 60 ns.

When helium is injected at the opposite end of the dielectric tube and the submicrosecond high voltage pulses are applied to the electrodes, a discharge is ignited in the gap between the electrodes and a plasma plume is launched through the hole of the outer electrode and in the surrounding room air.

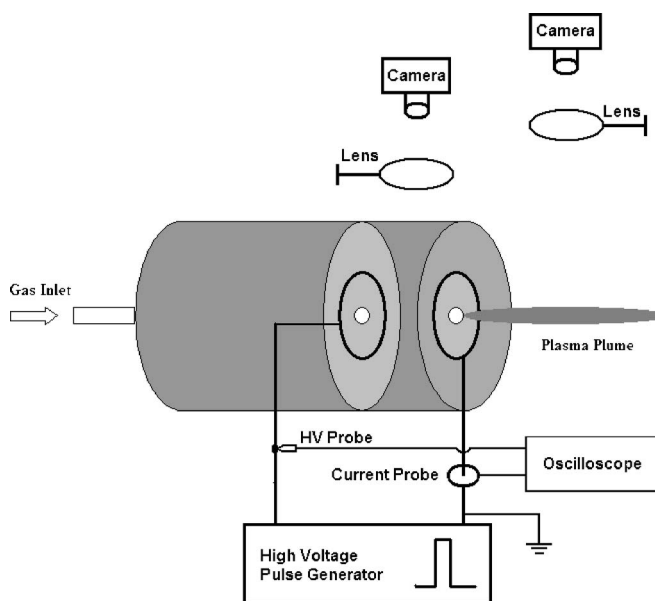


FIG. 1. Schematic of the experimental setup.

^{a)}Author to whom correspondence should be addressed; electronic mail: mlarouss@odu.edu

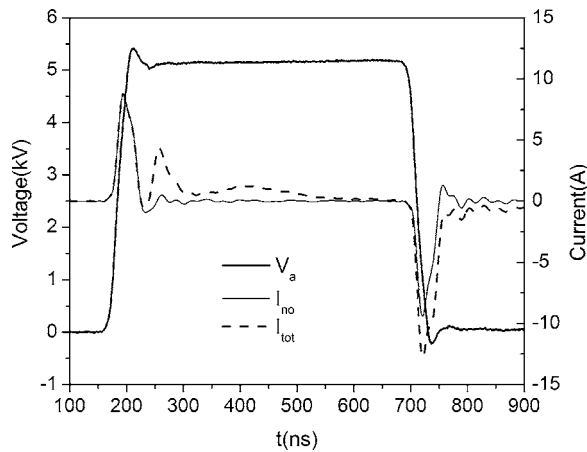


FIG. 2. Applied voltage V_a , total current I_{tot} , and displacement current I_{no} , vs time.

Applied voltages are measured by a P6015 Tektronix high voltage probe and currents by a A6312 Tektronix current probe. The voltage and current wave forms are viewed by a Tektronix TDS 784D wideband digital oscilloscope. A CCD camera (Stanford Computer Optics, Inc. Model 4 Picos) is used to capture the temporal and spatial behaviors of the discharge in the gap between the electrodes and of the plasma plume that is launched through the hole of the outer electrode.

EXPERIMENTAL RESULTS

For all the experimental results presented in this paper, the operating gas was helium and the applied voltage, pulse width, pulse frequency, and gap distance were $V_a=5$ kV, $t_{PW}=500$ ns, $f=1$ kHz, and $d=5$ mm, respectively. The helium gas flow rate was 3.5 min^{-1} .

The current-voltage characteristics of the discharge are shown in Fig. 2 and 3. Figure 2 shows the applied voltage V_a , displacement current I_{no} (without He flow: no plasma), and total current I_{tot} (with plasma on). It should be mentioned that the voltage wave form remains the same when the plasma is on or off. To find out the actual discharge current, the displacement current I_{no} is subtracted from the total current I_{tot} . Figure 3 shows the applied voltage V_a and actual

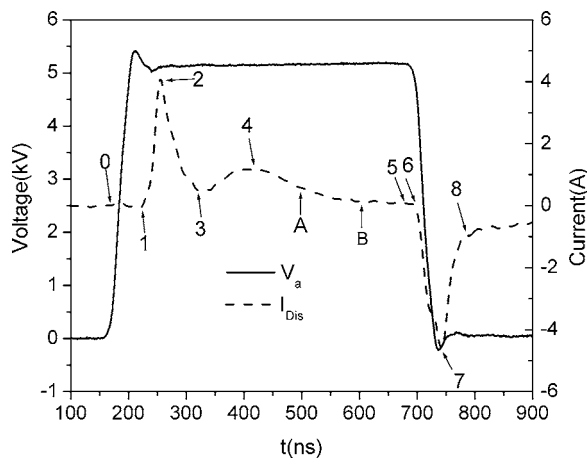


FIG. 3. Applied voltage V_a and discharge current I_{Dis} , vs time.

discharge current I_{dis} versus time. The first pulse of the discharge current starts after the applied voltage reaches its plateau value. The delay between the start of the applied voltage and that of the first discharge current pulse is about 60 ns. The first current pulse (between points 1 and 3) lasts about 100 ns. Immediately after the first current pulse, the discharge current has another increase. The peak value of this second current pulse is about one-fourth that of the first current pulse. But it lasts much longer (between points 3 and 6), about 375 ns. As can be seen, this second current pulse rises to a peak value of about 1.2 A in 100 ns (between points 3 and 4), then slowly decreases to zero in 275 ns (between points 4 and 6). It is interesting to note that this second current pulse was not observed in our planar dielectric barrier discharge driven by the same power supply¹¹ (this particular device did not emit a plume). The mechanism of this second current pulse, which is directly linked to the launch of the plume, will be discussed in the next section of this paper. After point 6, which is about 25 ns after the arrival of the falling front of the applied voltage (point 5), a third current pulse starts. This corresponds to a new breakdown of the gap. This discharge ignites because of the voltage induced by the charges, which have accumulated on the surface of the dielectric disk during the previous discharge.¹¹ This current pulse lasts about 100 ns, then decays to zero.

As we reported in Ref. 13, the plasma plume can achieve lengths of up to 5 cm. To better understand the dynamics of the plasma plume, and the evolution of the discharge inside the discharge chamber, a high-speed CCD camera with an exposure time of 50 ns is used to capture the temporal emission behavior of the plasma. In order to have a better spatial resolution of the discharge inside the chamber, the CCD camera and optical lens are adjusted to have a larger image of the discharge inside the chamber. Figures 4 and 5 show the temporal emission behavior of the discharge inside the chamber and that of the plasma plume in the open air, respectively. Photograph 4(a) was captured at the time corresponding to point 0 of Fig. 3 (170 ns). Photographs 4(b)–4(n) were taken at 50 ns increments. The plasma plume could only be captured by the CCD camera 320 ns after the start of the applied voltage pulse. This time corresponds to the time when photograph 4(d) was taken. To make Figs. 4 and 5 comparable, the first plasma plume photo of Fig. 5 is marked as (d). This means Figs. 5(d)–5(n) were taken at times corresponding to those of photographs 4(d)–4(n). Figure 5(o), on the other hand, was taken at point 0 with an exposure time of 700 ns, therefore showing the entire plume emission during a whole discharge pulse period.

Figure 4 shows the discharge current pulses and the corresponding photographs of the plasma inside the chamber. Each photograph was taken with an exposure time of 50 ns. Figure 5 shows a series of photographs starting from the time the plume could be captured [320 ns, the time corresponding to photograph (d) in Fig. 4]. Based on Figs. 4 and 5, there are interesting points worth emphasizing. First, as can be seen from photographs 4(b)–4(g), there is a dark layer of about 1.2 mm next to the cathode (right electrode), the rest of the

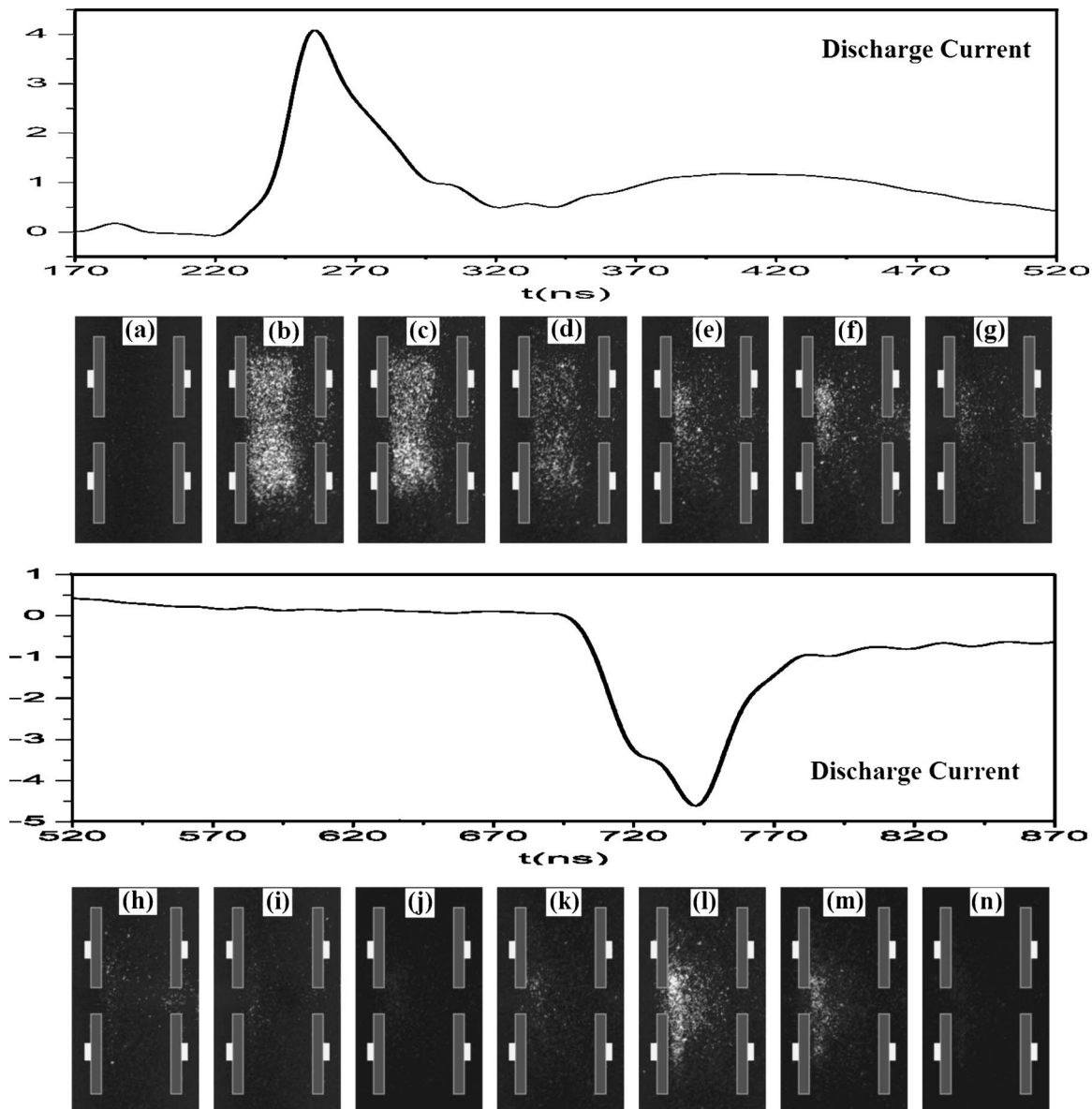


FIG. 4. High-speed photographs of the discharge inside the chamber and the corresponding discharge current. The exposure time of the photographs is 50 ns. Photograph (a) is taken at 170 ns and the rest at 50 ns increments. The gray bars on the left and right of each photograph represent the electrodes. Each electrode has a centrally located aperture, 3 mm in diameter. The plasma plume exits from the aperture on the right.

gap being dominated by homogeneous strong emission, which is similar to the Townsend-like discharge. Secondly, the plasma plume can be observed only after the second current pulse appeared.

To have a more detailed discussion about the plume dynamics, the plume velocity versus time is plotted in Fig. 6. Because the plume location has a small fluctuation for the same delay time, five photos are taken for every delay time. Figure 6 clearly shows that the plume starts to accelerate as soon as it is launched from the center hole of the outer electrode. It accelerates quickly and reaches about 1.4×10^5 m/s at a time corresponding to point A in Fig. 3. Then, with a lower acceleration, the plume velocity reaches its maximum value of about 1.5×10^5 m/s. This corresponds to point B in Fig. 3. Finally, the plume velocity drops quickly until it cannot be captured anymore.

DISCUSSION

As was mentioned earlier, the delay time between the start of the applied voltage pulse and that of the first discharge current pulse is about 60 ns. On the other hand, when the applied voltage starts falling, the charges accumulated on the dielectric induce a reverse voltage, which results in a third current pulse. The delay time between the arrival of the falling front of the applied voltage and the third current pulse is only 25 ns. This negative current pulse starts with a much lower voltage than that required for the initiation of the first current pulse. This lower voltage value is estimated to be about 1 kV. We attribute this to the presence of species, such as electrons, ions, and metastables, which are initially generated by the previous discharge (corresponding to the first and second current pulses). Since the third discharge current pulse occurs only few hundreds of nanoseconds after the first

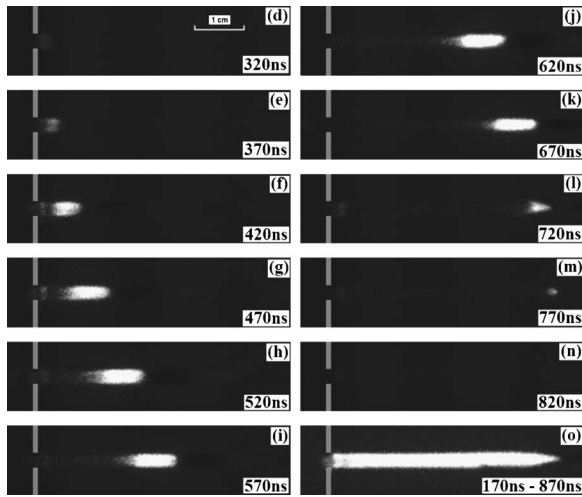


FIG. 5. High-speed photographs of the plasma plume/bullet. The exposure time is 50 ns. Photograph (d) is taken at 320 ns, the time corresponding to point 3 in Fig. 3. Photographs (e)–(n) are taken at 50 ns increments.

two pulses, the concentrations of some excited species, such as $N_2 B^3 \Pi_g$, $B^3 \Sigma_u^-$, $a^{n1} \Sigma_g^+$, and $D^3 \Sigma_u^+$ states and $N_2^+ A^2 \Pi_u$ states (which have a lifetime between microsecond and sub-microsecond ranges), should be higher than that when the first discharge starts. These states may contribute to the discharge corresponding to the third current pulse, but not to the primary discharge since their lifetime is too short compared to the time between the applied voltage pulses (which is typically several hundreds of microseconds long.)

The second current pulse is related to the launch of the plasma plume. There are two evidences that support this assumption. First, the plasma plume exits the center hole of the outer electrode at the same time when the second current pulse starts. Secondly, when the second current pulse starts (corresponding to point 3 in Fig. 3), the high-speed photograph of Fig. 4(d) shows that the emission intensity from the chamber does not increase at all. In fact, it decreases. Besides, it should be pointed out that the emission intensity from inside the chamber decays slower after the first current pulse than that after the third current pulse, as can be seen from photographs 4(d)–4(i) and 4(m) and 4(n). As a result,

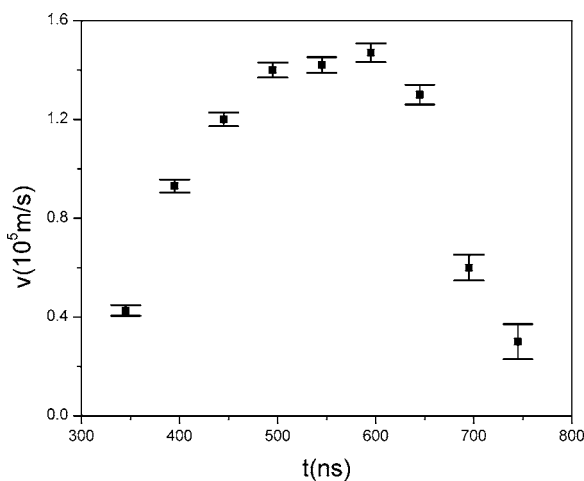


FIG. 6. Velocity of the "plasma bullet" vs time.

we think that part of the second current pulse contributes to the plasma plume and the rest is related to the discharge inside the chamber.

It is interesting to note that the maximum value of the plasma plume velocity is in the order of 10^5 m/s, a much greater value than the gas velocity of 8.3 m/s, as calculated according to the gas flow rate and the diameter of the hole. To have a better understanding of the mechanism of plume dynamics, first, the electron drift velocities inside the chamber and along the plasma plume are estimated. The product of pressure p and mobility of electron μ_e in pure He is 0.86×10^6 cm² Torr/V s.¹⁴ For our case, the pressure p is 760 Torr, the applied voltage V_a is 5 kV, and the gap distance d is 5 mm. So the electron drift velocity v_e can be estimated by $v_e = \mu_e E$, which is about 1.1×10^5 m/s. It is within the same order of magnitude as the plume velocity. However, the plume is propagating outside the discharge chamber, where the electric field is much lower than that inside the chamber. Even if the electric field is assumed to be uniform from the center of the high voltage electrode to the tip of the plume, the maximum drift velocity that the electron could achieve along the plume is only about 1.1×10^4 m/s, which is one order of magnitude less than the plume velocity. In this estimation, we assume that the background gas is pure helium. If an air impurity is considered, then the electron drift velocity will be even lower because the mobility of electrons μ_e will be smaller in the presence of air.

According to the emission spectrum of the plasma,¹³ the dominant ion is N_2^+ . So the drift velocity of N_2^+ is calculated as follows: The mobility of N_2^+ in pure He at atmospheric pressure is about 23 cm²/V s.¹⁵ Based on the same assumption used for calculating the electron drift velocity inside the chamber and in the plume, the N_2^+ drift velocities inside the discharge chamber and in the plume are 2.3×10^3 and 2.2×10^2 m/s, respectively. These speeds are far slower (up to three orders of magnitudes) than the measured plume velocity.

None of the mechanisms discussed above provides an adequate explanation on why the plume propagation velocity is as high as it is. We therefore propose the following explanation: To have a plume/bullet travel in such high speed under very low electric field, photoionization has to play an important role. Dawson and Winn¹⁶ proposed a streamer propagation model in low electric field based on a photoionization assumption. In their model, the head of a cathode-directed streamer is a sphere of radius r_0 , containing n^+ positive ions. As it moves forward, it leaves behind a quasineutral ionized channel with a negligibly low conductivity; the head is not connected to the anode and only the streamer head is measurably luminous. This is exactly what is happening in our case. As can be seen in Fig. 5, the emission from the track left by the plasma plume is very weak. We therefore propose the following model.

Assume that at a given instant of time, the streamer head consists of a small sphere, which has a radius r_0 and a space charge n^+ . Because of photon emission from the streamer, suppose that a single photoelectron is created at a suitable distance r_1 from the center of the sphere, as shown in Fig. 7. Under the influence of the field set up by the space charge,

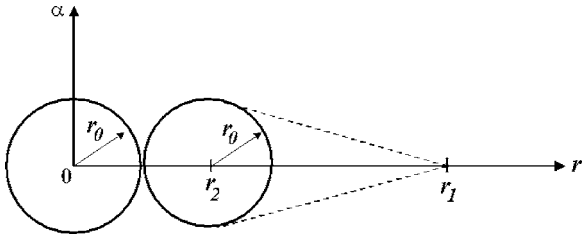


FIG. 7. Schematic illustrating the streamer propagation model described in this paper.

the electron is accelerated towards the sphere and an avalanche is initiated. In moving toward the sphere, from r_1 up to some point r_2 , the electron forms an avalanche of multiplication

$$n = \exp \int_{r_2}^{r_1} \alpha dr, \quad (1)$$

and of diffusion radius

$$r_0 = \left(6 \int_{r_2}^{r_1} \frac{D}{v_d} dr \right)^{1/2}, \quad (2)$$

where α is Townsend's first ionization coefficient, D is the diffusion coefficient, and v_d is the electron drift velocity. If the multiplication up to the sphere is sufficient, the electrons neutralize the positive charge but leave behind a new positive region. The best value of r_1 could, in principle, be obtained from an exact knowledge of the number and type of photons emitted from the sphere within a particular solid angle, their absorption coefficients, and ionizing efficiency. Since complete data on these quantities are not available, r_1 is taken as the distance at which the electric field strength is such that ionization and attachment rates become equal. For air, this occurs when $E/p=30$ V/cm mmHg.¹⁶

According to Ref. 16, the following three requirements must be fulfilled in order for the streamer propagation under low or zero field to occur: (1) The number of new positive ions created by the avalanche must be equal to n^+ , the number of ions in the original sphere; (2) the diffusion radius of the avalanche head must not become larger than r_0 ; and (3) the avalanche must reach the required amplification before the two charge regions begin to overlap, i.e., $2r_0 \leq r_2$.

Next, r_2 and r_0 are calculated for different values of positive charge n^+ . The procedure is as follows: First, a value of n^+ is given. Second, the electric field as a function of r from simple electrostatics is calculated according to

$$E = \frac{Q}{4\pi\epsilon_0 r^2}. \quad (3)$$

Here, although the main gas is helium, the main ion is N_2^+ Ref. 13 (nitrogen originates from the surrounding air). In addition, the attachment process is dominated by O_2 , also from air, which diffuses to the plume. Since the percentage (per volume) of air in the plume is not readily known, we assume that it is about 1%. The distance r_1 is determined as the distance at which the reduced electric field is equal to 30 V/cm mmHg.¹⁶ Then, r_2 is calculated according to Eq.

TABLE I. Calculated radii (r_0 and r_2) for different original space charge numbers.

n^+ (Number of original positive charges) (10^9)	1	2	3	4	5
r_2 (cm)	0.02	0.1	0.17	0.23	0.3
r_0 (cm)	0.056	0.068	0.075	0.080	0.085

(1) when n is equal to n^+ . Townsend's first ionization coefficient α is calculated according to¹⁴

$$\alpha = 15p \exp(-365p/E) \text{cm}^{-1}, \quad (4)$$

where p is the pressure and air is assumed to be the background gas (this assumption, of course, introduces an error since the helium metastable state plays an important role in the ionization process.) Finally, by using Eq. (2), r_0 is calculated, where D and μ_e were determined according to¹⁴

$$D = \frac{2 \times 10^5}{p(\text{Torr})} \text{cm}^2/\text{s}, \quad (5)$$

$$\mu_e = \frac{0.86 \times 10^6}{p(\text{Torr})} \text{cm}^2/\text{V s}. \quad (6)$$

Table I shows the calculated r_2 and r_0 for different n^+ . In these calculations, the values of D and v_d were determined for the case of helium gas. The three requirements for the streamer self-propagation are met only if $2r_0$ is smaller than r_2 . From Table I, it can be seen that when n^+ is less than 2×10^9 , $2r_0$ is greater than r_2 . This means that the streamer head cannot self-propagate under this condition. However, when n^+ is larger than 3×10^9 , $2r_0$ is smaller than r_2 , meaning that the streamer head can self-propagate under low or zero external electric field. Therefore, according to Dawson and Winn,¹⁶ the plume velocity can reach values as high as 10^6 m/s and it can travel up to several centimeters without the presence of an external electric field. This is in agreement with our experimental observations.

It should be emphasized here that energy is needed for the ionization of the new volume of gas replaced by the streamer channel. This energy can be drawn only from an external source. Therefore, the self-propagation streamer model in low applied electric field discussed above is not steady but merely a quasi-steady-state process. The streamer will stop propagating when the electrostatic energy of the sphere of charges is lost via the ionization processes. Detailed description of how a cathode directed streamer stops propagating can be found in Ref. 16.

CONCLUSIONS

A cold plasma plume traveling with a speed of up to 10^5 m/s is reported. The I - V characteristics show that for each applied voltage pulse there are three consecutive discharge pulses. The first pulse is associated with a first discharge initiation, the second current pulse is linked to the launch of the plasma plume, and the third current pulse is associated with a discharge caused by the charge buildup on the dielectric surfaces of the electrodes. A mechanism of the

plume traveling at high speeds but under very low electric field is proposed and discussed. A streamer model based on photoionization is used to explain this interesting phenomenon. Fast photography shows that the plume is more like a bullet formed by a small and well-confined plasma volume that travels from the exit aperture of the device and terminates at some distance in the surrounding air. However, how this bulletlike plasma accelerates and how it stops is still not quite clear.

ACKNOWLEDGMENT

This work was partly supported by a grant from AFOSR.

¹M. Laroussi, *Plasma Processes Polym.* **2**, 391 (2005).

²Z. Machala, E. Marode, M. Morvova, and P. Lukac, *Plasma Processes*

Polym. **2**, 152 (2005).

³R. Dorai and M. J. Kushner, *J. Phys. D* **36**, 666 (2003).

⁴R. Vidmar, *IEEE Trans. Plasma Sci.* **18**, 733 (1990).

⁵M. Laroussi, *Int. J. Infrared Millim. Waves* **16**, 2069 (1995).

⁶H. E. Wagner, R. Brandenburg, K. V. Kozlov, A. Sonnenfeld, P. Michel, and J. F. Behnke, *Vacuum* **71**, 417 (2003).

⁷F. Massines and G. Gouda, *J. Phys. D* **31**, 3411 (1998).

⁸K. Ostrikov, *Rev. Mod. Phys.* **77**, 489 (2005).

⁹S. Liu and M. Neiger, *J. Phys. D* **34**, 1632 (2001).

¹⁰R. P. Mildren, R. J. Carman, and I. S. Falconer, *J. Phys. D* **34**, 3378 (2001).

¹¹M. Laroussi, X. Lu, V. Kolobov, and R. Arslanbekov, *J. Appl. Phys.* **96**, 3028 (2004).

¹²X. Lu and M. Laroussi, *J. Appl. Phys.* **98**, 023301 (2005).

¹³M. Laroussi and X. Lu, *Appl. Phys. Lett.* **87**, 113902 (2005).

¹⁴R. P. Yuri, *Gas Discharge Physics* (Springer-Verlag, New York, 1991).

¹⁵B. Sanborn, *Basic Data of Plasma Physics* (AIP, New York, 1993).

¹⁶G. A. Dawson and W. P. Winn, *Z. Phys.* **183**, 159 (1965).